Numerical prediction for resistance of Canadian icebreaker CCGS Terry Fox in level ice

Wang, Jungyong; Derradji-Aouat, Ahmed

National Research Council Canada   Conseil national de recherches Canada

Canada

Numerical Prediction for Resistance of Canadian Icebreaker CCGS Terry Fox in Level Ice

Jungyong Wang, Institute for Ocean Technology, National Research Council, Canada
Ahmed Derradji-Aouat, Institute for Ocean Technology, National Research Council, Canada

SUMMARY

The aim of this paper is to present numerical prediction results for an icebreaker resistance in level ice. Two commercial finite element codes (ANSYS and LS-DYNA) are used. ANSYS is used for a pre-processor and it enables us to generate an adequate mesh for an explicit solver, LS-DYNA. In LS-DYNA, a user-defined material routine is used to simulate ice: a multi-surface failure criterion is implemented and ice behaves as a liner elastic material before a failure occurs. Wang and Derradji (2009) showed the detailed implementation procedure and validation of the code. Numerical results are then compared to full-scale measurement results. As an ultimate goal, model tests and numerical predictions are to be complementary each other to provide accurate evaluation for a full-scale performance. A detailed numerical scheme is explained and results are discussed.

NOMENCLATURE

$\dot{\varepsilon}$	Strain rate (1/s)
τ_{oct}	Octahedral shear stress (Pa)
P	Hydrostatic pressure (Pa)
T	Temperature (°C)
V	Ship speed (m/s)

1. INTRODUCTION

As interest in Arctic transportation increases in recent years, the number of ice model testing and numerical simulation of ships and structures have been increased for optimum design and operation in ice-covered waters. Since ice is a complicated material for numerical modeling, model tests in ice tank have been preferred. An accurate numerical modeling, however, provides invaluable information such as local ice pressure and pressure distribution of ice and enables us to simulate extreme operating scenarios which would be beyond the scope of model testing. It also significantly saves the cost compared to model testing, especially for a parametric study. Numerical simulation is not an alternative of model testing, but is complementary.

National Research Council (NRC)'s Institute for Ocean Technology (IOT) was established in 1985 and since then IOT produced more than 1200 ice sheets for model testing in its ice tank. One of the Canadian icebreaker models, Terry Fox has been tested since 1988 and the recent tests were carried out in 2007. Wang and Jones (2008) re-collected all the model test data and two sets of full-scale measurement data and compared each other, which showed a good agreement. For details of the full-scale measurement and model test, see Wang and Jones (2008). Numerical simulation results are compared to model test and full-scale measurement, and discussed in this paper.

For the simulation of a ship in level ice, the ice needs to be modeled but there is no default material model for ice in any commercial software such as ANSYS and LS-DYNA. One of the methods for ice modeling is to use ice failure envelope based on ice failure characteristics. Ice failure envelopes were proposed by several researchers (Wang, 1979; Nadreau and Michel, 1986; Fish, 1997; Schulson, 2001; Derradji-Aouat, 2003). Most failure envelopes consider the effect of strain rate, temperature, and hydrostatic pressure. In particular, Derradji-Aouat (2003) compiled published triaxial compression test data and proposed the 3-D ellipsoidal failure envelope and this envelope has been modified and implemented in LS-DYNA using a user-defined material (Wang and Derradji-Aouat, 2009). Because the data from triaxial compression tests was used, the weakest part of the model is criteria in extension (tensile, bending) condition. When a ship breaks level ice, however, the dominant failure mode is flexural bending and the flexural strength of the target ice has to be considered. In this paper, flexural bending failure of ice was included in the failure envelope and the detailed procedure is presented. After the failure envelope was determined at each ship speed, the simulation of a ship in level ice was carried out.

Detailed description for this finite element model including mesh generation was published by Derradji-Aouat (2006) and his FE model was a starting point for the present paper. Technical issues such as Arbitrary Lagrangian-Eulerian (ALE) modeling, Coupling and Contact in LS-DYNA were described in his paper.

2. FAILURE CRITERION FOR ICE

In this study, ice failure envelope suggested by Derradji-Aouat (2003) is implemented and simulated in LS-DYNA. A detailed implementation procedure was published by Wang and Derradji-Aouat (2009). The

envelope formulation has been modified and the final equations for sea ice are presented as below.

In 2-D, the failure criteria for freshwater ice and saline ice are shown in Fig. 1. The failure envelope is a function of hydrostatic pressure and octahedral shear stress and it forms elliptic shape (Eq. 1).
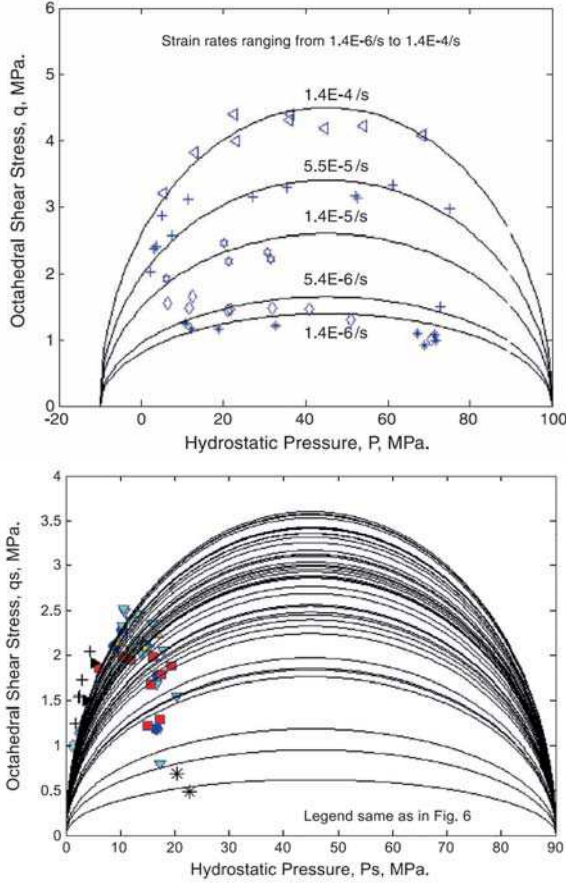

Figure 1: Elliptic failure envelope from triaxial compression tests for freshwater (top) and saline (bottom) ice (from Derradji-Aouat, 2003)

$$\left(\frac{\tau_{oct} - \eta}{\tau_{oct\_max}}\right) + \left(\frac{p - \lambda}{P_{c\_max}}\right) = 1 \qquad (1)$$

where τ_{oct} and p are the octahedral shear stress in the minor axis and hydrostatic pressure (same as the confining pressure, P_c) in the major axis, and η and λ are the coordinates for the center of the ellipse. In a typical triaxial test, lateral pressure at two axes (x-2 and x-3) was the same as the confining pressure P_c, i.e. $\sigma_2 = \sigma_3 = P_c$ (see Fig. 2). Therefore, Eq. 1 can be extended to the 3-D, which is a circular ellipsoid and the general equation is shown in Eq. 2.
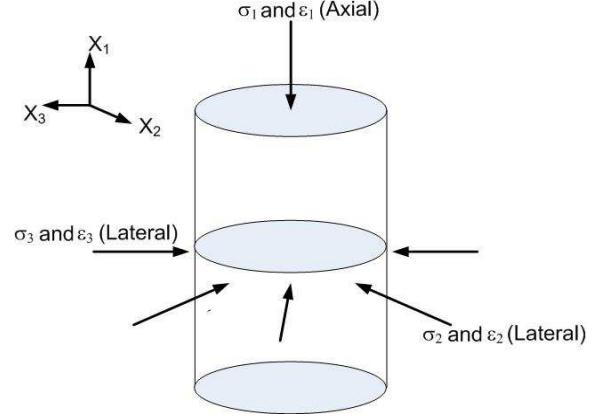

Figure 2: A schematic of triaxial loading direction

$$\left(\frac{(p^* - \alpha)}{a}\right)^2 + \left(\frac{(s - \beta)}{b}\right)^2 + \left(\frac{(s' - \gamma)}{c}\right)^2 = 1 \qquad (2)$$

where $a = P_{c\_max}$ (45MPa for saline ice and 55MPa for freshwater/iceberg ice) , $b = c = \tau_{oct\_max}$, and $\alpha = \lambda = 45MPa$.

The apex of octahedral shear stress was formulated based on the test results from tri-axial compression tests and the equation is shown in Eq. 3. The centre of hydrostatic pressure, which is 45 MPa, was also estimated.

$$\tau_{oct\_max} = \left(\frac{\dot{\varepsilon}}{\xi}\right)^{1/n} \qquad (3)$$

where

$$n = 4, \ \xi = 5 \times 10^{-6} \exp\left[-10.5 \times 10^3 \left(\frac{1}{T} - \frac{1}{273}\right)\right]$$

Since ice failure is dependent on the strain rate ($\dot{\varepsilon}$), empirical formula of $V/4D$ is used; where V is the ship speed and D is the maximum beam of the ship (Cammaert and Muggeridge, 1998).

Eq. 2 can be re-written as an invariant form as shown in Eq. 4.

$$\frac{8}{3b^2}J_{2D} + \frac{2}{3b^2}I_2 + \left(\frac{1}{9a^2} - \frac{2}{9b^2}\right)I_1^2 + \frac{2\alpha}{3a^2}I_1 + \frac{\alpha^2}{a^2} = 1 \ (4)$$

where, I_1, I_2, and J_{2D} are the first, second stress invariants, and the second deviatoric stress invariants. Other parameters are the same as those in Eq. 2. Full derivation was reported by Wang and Derradji-Aouat (2009), but some modification was made in this paper. In the invariant form, Eq. 4 is always valid regardless a coordinate system. Eq. 4 indicates that if the value from the left hand side is equal or bigger than 1, then the element reaches the failure.

In this paper, we used the formulation for the saline ice, but it gave only positive hydrostatic pressure term, which meant the failure considered only under the compression condition. Since the flexural bending failure will be a dominant failure mode for the present "ship in level ice" simulation, this failure envelope needs to be modified and includes bending condition. However, due to the lack of database for extension tests for ice, the negative axis-intercept of the hydrostatic pressure was determined numerically. In order to do this, cantilever beam failure was simulated prior to the ship in ice simulation. Then the failure envelope was numerically calibrated based on the particular flexural strength of the target ice.

3.   CANTILEVER BEAM FAILURE

Flexural strength of ice is dependant on the effects of brine content, crystal size, temperature, sample size and strain rate (Williams, 1993). Therefore, it would be hard to identify the flexural strength of ice accurately unless all these parameters were reported. From the full-scale measurement carried out 1991, flexural strength of the ice was reported as 150 kPa but this number was too low possibly related to the operational difficulties. Since they measured salinity and temperature, which were 2.5 ~ 4 ppt and 1.4 ~ -2.3°C, respectively, the flexural strength was estimated by using the various formulas (based on the brine volume) and chart given by Cammaert and Muggeridge (1988) and Timco and O'Brien (1994). The range of the estimated flexural strength would be 300 ~ 600 KPa, and 600 KPa was used in this study.

For an input deck in LS-DYNA, all material properties need to be specified. For the ice sheet, an elasto-plastic material was used. The density of 914kg/m^3 was used. The reported elastic modulus from the full-scale measurements had two wide ranges; 1-5 Gpa from dynamic measurement and 0.1-0.5 Gpa from static measurement method. Wang and Lau (2007) reviewed the ratio between Young's modulus and a flexural strength, which is from 2000 to 8000 for a sea ice. The elastic is then estimated as 1.5 GPa based on the ratio of 2500.

From Eq. 1, a is substituted by $a+a_1$ and a_1 is the negative p-axis-intercept (see Eq. 5).

$$\left(\frac{(p^*-\alpha)}{a+a_1}\right)^2+\left(\frac{(s-\beta)}{b}\right)^2+\left(\frac{(s'-\gamma)}{c}\right)^2=1 \qquad (5)$$

Fig. 3 is the sketch of the failure envelope for one of the target speeds of the ship. In the right in Fig. 3, it shows the negative p-axis-intercept. Again the negative hydrostatic pressure (p) means the ice is under the extension condition.
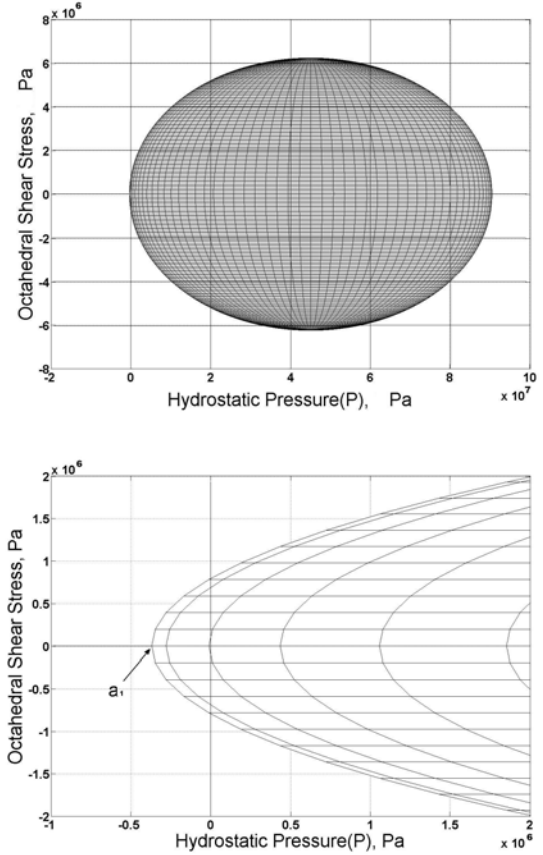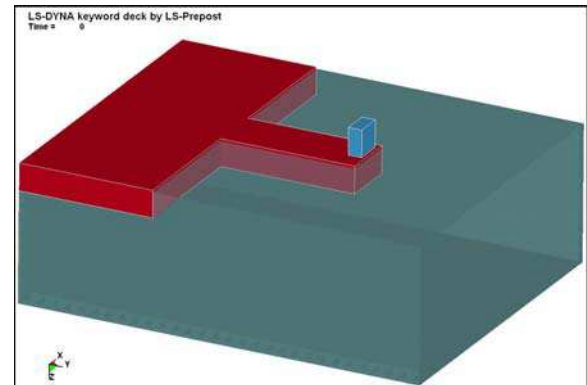

Figure 3: Failure envelop for V = 2.4 knots

Fig. 4 shows the set-up for the numerical model and effective stress distribution. A red T-shaped material (cantilever beam) is the ice which is floating on the water and a rigid indentor (blue) is located at the tip of and above the ice. After the hydrostatic pressure of the water stabilized, the rigid indentor moved down and pushed the ice tip downward. Stress concentration was found at the fixed end of the cantilever beam where the failure occurred. The hydrostatic pressure of the ice element where the failure occurred was about -0.2 MPa and the effective stress for the flexural failure was 0.59MPa (Fig. 5).
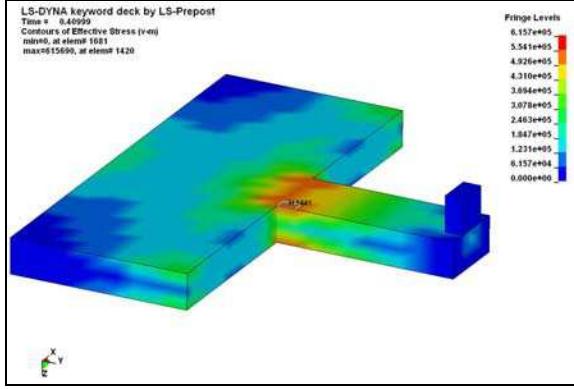
Figure 4: Numerical model set-up (top) and effective stress distribution before failure (bottom)
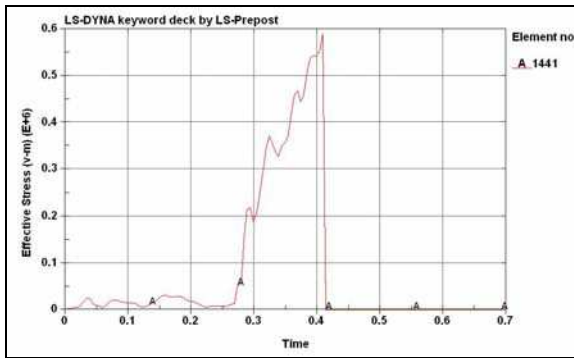

Figure 5: Effective stress of one element which was failed at the fixed end of the cantilever beam

Table 1 shows the a_1 for each ship speed. Since the maximum octahedral shear stress (τ_{oct_max}) was the function of temperature and strain rate (see Eq. 3), each envelope had to have proper negative p-axis-intercepts (a_1) value to match a target flexural strength. In this study, the parametric calculation (range of a_1 value was from 0.1 to 0.6 MPa) was performed, and a_1 values were determined when the failure stress was close to 0.6 MPa (target flexural strength). The failure stress was the maximum effective stress from one element in the failed area, which was the fixed end of the cantilever beam.

Table 1: Numerical calibration of failure envelope for the flexural failure (Target flexural strength = 0.6 *MPa*)

Ship speed (knots)	Strain rate (1/s)	τ_{oct_max} *(MPa)*	a_1 (MPa)	Failure Stress *(MPa)*
0.4	0.006	6.23	0.37	0.59
2.4	0.03	9.69	0.28	0.59
3.3	0.05	10.51	0.25	0.59

4.   Numerical Simulation for Ship in Level Ice

Failure envelopes for each ship speeds were established by using cantilever beam failure simulation as mentioned previously. Two sets of numerical models were used; half-modeling of ship/ice/water/air with symmetric condition, and full-modeling of ship/ice without water/air. It is noted that the usage of Arbitrary Lagrangian-Eulerian (ALE) means the interaction between a Lagrangian material set (ship and ice) and Eulerian material set (water and air) is considered. Ship was modeled as a rigid body and ice was an elastic material with the failure envelope. When the ice element reaches the failure criterion, the element was set to be eroded. Ice was free to float in z-direction. Frictional coefficient of 0.18 (between ship and ice) was used, which was measured from the full-scale measurement (Cowper, 1991).

- HALF MODELING WITH ALE AND SYMMETRIC CONDITION

By using the symmetric condition, only half of the ship/ice/water/air was modelled and the total element number was about 110,000 in order to keep a reasonable simulation time, which is about 1-2 days.
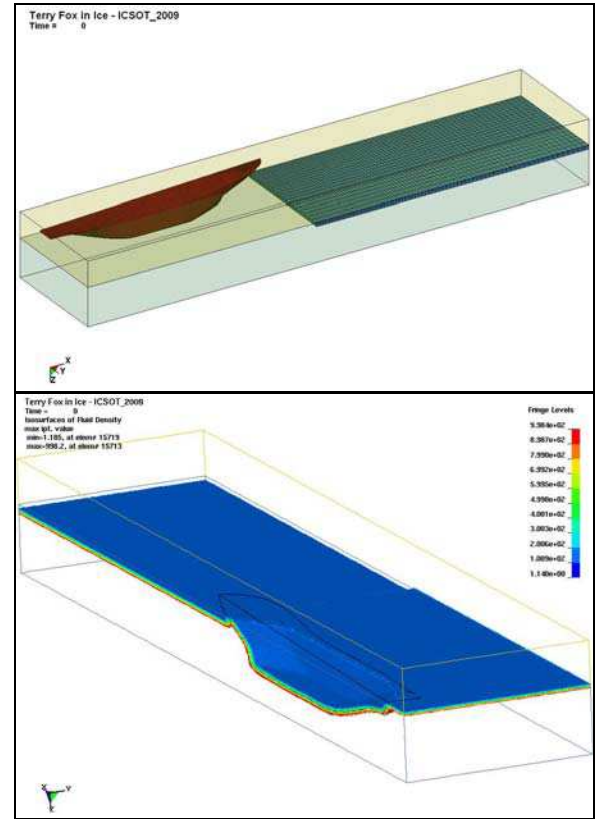

Figure 6: Half modeling with symmetric condition (top) and initial density contour (bottom)

Fig.6 shows the initial status for the simulation (top) and the density contour (bottom). In the opposite side of

symmetric boundary, far front side and the bottom, non-reflecting boundary conditions were applied to represent infinite boundary conditions.

For the second speed (V = 2.4 knots), simulated breaking patterns are shown in Fig. 7. From the contact between the ship and ice, the reaction force of the ice was recorded. The total ice forces are then multiplied by 2 because of half-modeling. Unfortunately the Fluid-Structure Interaction (FSI) part (ship and water) is not properly coupled, the water resistance was not measured from the present calculation. From the model test data (Wang and Jones, 2007) open water resistance was estimated as up to 0.03MPa (at the highest speed) but this value was not included in the results.

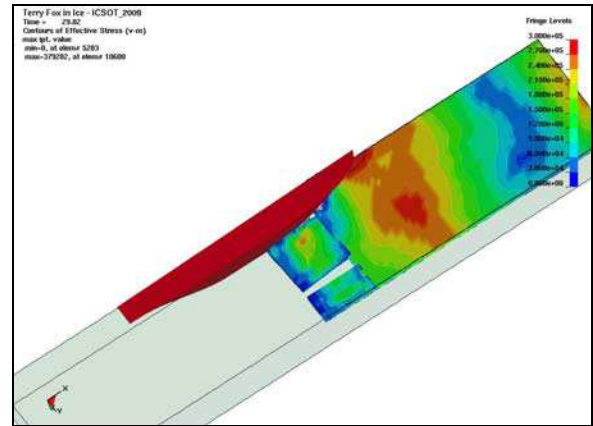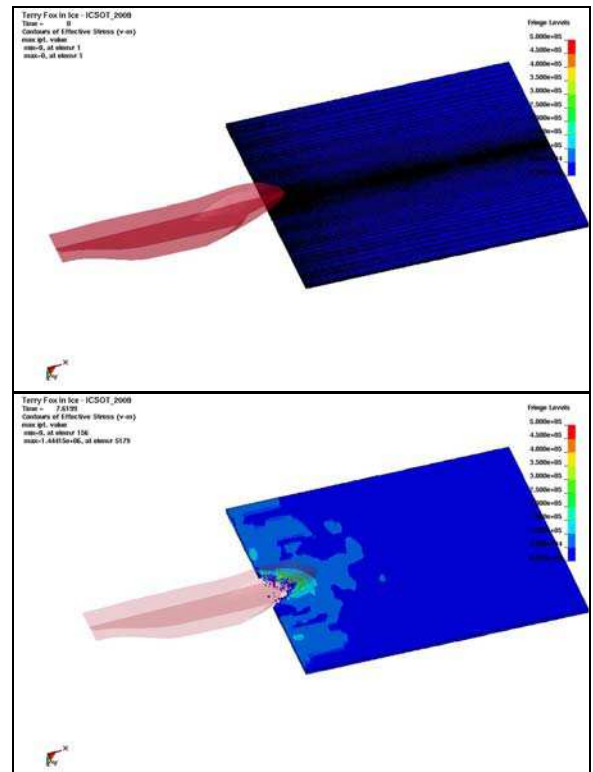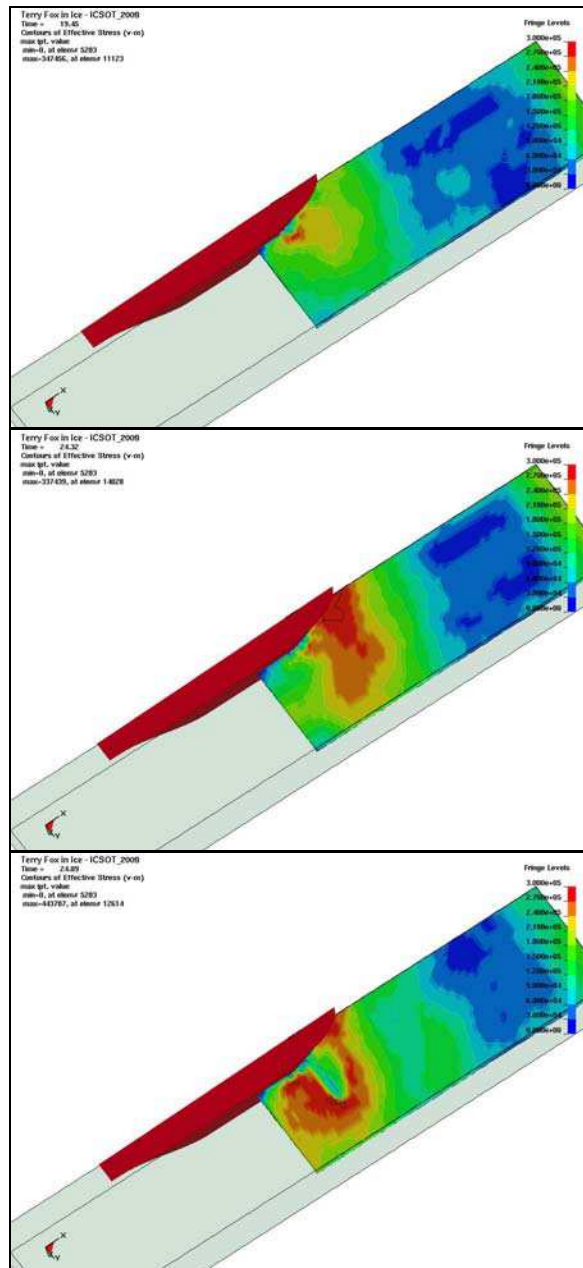
Figure: 7 Simulated breaking pattern for V=2.4 knots (from top to bottom)

- FULL MODELING WITHOUT ALE

Total number of element for this simulation was 57,000 and water/air were not included. Ice was fixed at each boundary (both sides and back). In Fig. 8, initial numerical model set up is shown at the top. A consequent ice-breaking pattern is shown in the Fig. 8.
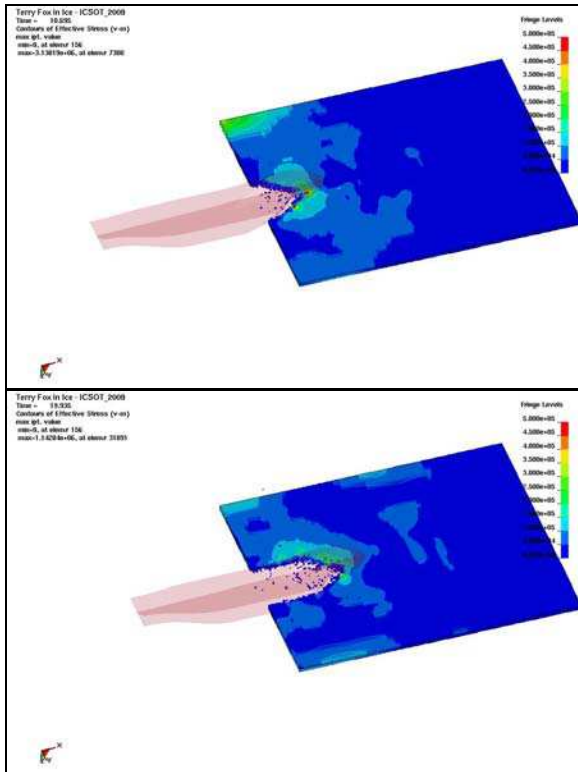
Figure 8: Full modeling without ALE

Table 2 shows the comparison between full-scale measurement and numerical prediction with/without ALE. The results from the simulation of half-modeling with ALE are encouraging. For the half-modeling case, the total number of elements was somewhat limited due to the calculation time and water/air parts need to be modeled. Consequently the size of ice elements was quite big to use the eroding failure treatment. This causes that when the element reached the failure stress and was eroded, the total reaction force was frequently drop to zero.

During the data manipulation process, zero values were excluded to calculate the average value and only data after a transient period were considered. In this paper, the transient period was defined as the time before the shoulder of the ship contacted the ice. The transient periods for three speeds (0.4, 2.4, 3.3 knots) were 30, 15, and 10 sec, respectively (See Fig. 9). It is noted that for the slowest speed (0.4 knots), total simulation time was 60 sec, while others were 30 sec.

Total resistance in ice would be composed of four terms which are breaking, clearing, buoyancy and open water resistance terms (Wang and Jones, 2008). In this simulation, some of clearing/buoyancy resistance may not be considered when the element reached the failure stress and eroded. The shortfall of 0.1~0.2MN in Table 2 would be explained by the effect of eroded elements. It was also reported that in the full-scale measurement some data was excluded if there was a large crack to the

open water and resulting pressure relief. In this simulation, data within a large crack (especially at high speed) were also taken into account, which may support this shortfall.

From the comparison of two numerical modeling (with/without ALE), it is found that water plays an important role in the simulation. Water supports the ice sheet with buoyancy force and it can result in an appropriate flexural bending failure. In the full-modeling without ALE, the calculated reaction forces from ice were lower than both full scale measurement and half modeling with ALE (Table 2). Since this simulation didn't include ALE, ice failed by insufficient force due to large bending. At the higher speed, ice breaking force was reduced which is possibly because the larger vicinity of the contact area from bow had been eroded due to impact and higher bending caused by the absence of water.

Table 2: Comparison between full-scale measurement and numerical prediction with/without ALE

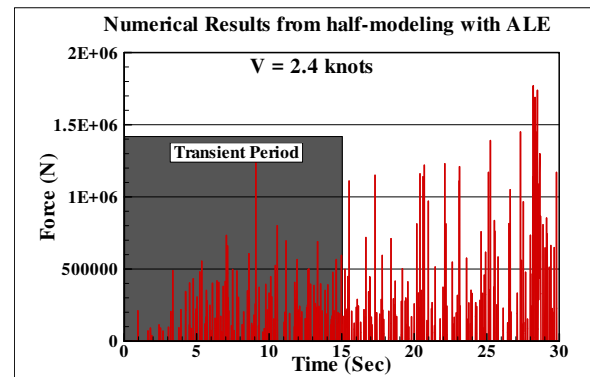| Ship Speed	Full-Scale Measure-ment	Half-Modeling with ALE	Full-Modeling without ALE
0.4 Knots (0.21 m/s)	0.42 MN	0.22 MN	0.30 MN
2.4 Knots (1.23 m/s)	0.83 MN	0.73 MN	0.53 MN
3.3 knots (1.70 m/s)	0.95 MN	0.83 MN	0.40 MN

Figure 9: Numerical results – total force at V= 2.4 Knots

5   CONCLUSION

This paper shows the numerical simulation for the resistance of an icebreaker navigating in level ice. For ice modeling, the ice failure envelope was modified to include the extension condition to simulate flexural bending, and implemented into LS-DYNA. Prior to simulation of the ship, a cantilever beam failure was simulated to determine the failure envelope corresponding to each ship speed and flexural strength of ice.

The numerical result from full-modeling without ALE shows that the water plays an important role in the whole simulation because it provides a buoyancy force and acts as a damper for bending failure of ice. Therefore the numerical modeling should include the interaction between Lagrangian parts (ship and ice) and Eulerian parts (water and air) which is called ALE.

The results from the simulation of half-modeling with ALE are very encouraging. Implemented failure envelope provided a reasonable load and failure pattern. The presented FE modeling method will be very useful for ship design with regard to performance evaluation of ships in ice.

Some recommendations for the future works are addressed below.

- For the failure treatment, this study used the element eroding method. If the element size is not small enough, then the calculated load may be underestimated. Broken ice pieces also may not be simulated properly. Denser mesh (increase element number) would be necessary. Other failure treatment method such as node-release method might be a better option.

- As a user defined material at the current version in LS-DYNA, this simulation couldn't run on the cluster which is designed for MPP (Massively Parallel). The user defined material needs to be optimized.

- Friction coefficient between ship and ice plays an important role in the total ice resistance, so that the parametric study for friction needs to be done.

6.   REFERENCES

1. Cammaert, A. and Muggeridge, D., ' Ice Interaction with Offshore Structures,' New York, Van Nostrand Reinhold, pp. 432, 1988.

2. Cowper, B., 'Resistance and Propulsive performance Trials of the MV Terry Fox and MV Ikaluk in level Ice,' Transport Canada, Report Number TP10845E, 1991.

3. Derradji-Aouat, A., 'Multi-Surface Failure Criterion for Saline Ice in the Brittle Regime,' Cold Regions Science and Technology, Vol. 36, pp. 47-70, 2003.

4. Derradj-Aouat, A., 'Ships in Ice-Solution from an Enhanced Finite Element Methodology, Part I – Numerical Development and Modeling Philosophy,' Proc. Of the 21st International Symposium on Okhotsk Sea & Sea Ice, Mombetsu, Hokkaido, Japan, pp. 67-72, 2006.

5. Fish, A., 'Ice Strength as a Function of Hydrostatic Pressure and Temperature,'' Cold Regions Research and engineering lab hanover, NH, 1997.

6. Nadreau, J. P. and Michel, B., 'Yield and Failure Envelope for Ice under Multiaxial Compressive Stresses,' Cold Regions Science and Technology, Vol. 13, pp. 75-82, 1986.

7. Schulson, E. M., 'Brittle Failure of Ice,' Engineering Fracture Mechanics, Vol. 68, pp. 1839-1887, 2001.

8. Timco, G. and O'Brien, S., 'Flexural Strength Equation for Sea Ice,' Cold Regions Science and Technology, Vol. 22, pp. 285-298, 1994.

9. Wang, J. and Lau, M., 'A state-of-the-art Review on Ice Modeling Methodologies Employed in Refrigerated Ice Tanks,' Institute for Ocean Technology, LM-2007-05, St. John's, Canada, pp.37, 2007.

10. Wang, J. and Jones, S. J., 'Resistance and Propulsion of CCGS *Terry Fox* in Ice from Model Tests to Full Scale Correlation,' Proc. of the International Conference and Exhibition on Performance and Structures in ice (ICETECH 08), July 20-23, Banff, Canada, 2008.

11. Wang, J. and Derradji-Aouat, A., 'Implementation, Verification and Validation of the Multi-Surface Failure Envelope for Ice in Explicit FEA,' POAC09, June 9-12, Lulea, Sweden, 2009.

12. Wang, Y., 'Sea Ice Properties,' In Technical Seminar on Alaskan Beaufort Gravel Island Design, Exxon, USA, 1979.

13. Williams, F. M., 'Database: Flexural Strength of Ice Over Five Parameters,' Institute for Ocean Technology, LM-1993-32, St. John's, Canada, 1993.

7.   AUTHORS BIOGRAPHY

Jungyong Wang holds the current position of Research Officer at the National Research Council's Institute for Ocean Technology at St. John's, Canada. He is responsible for Arctic Engineering including experiments and numerical modeling for ships and structures in ice covered waters. Jungyong.Wang@nrc-cnrc.gc.ca

Ahmed Derradji-Aouat is a senior research officer at the National Research Council's Institute for Ocean Technology at St. John's, Canada. Leads projects related to arctic offshore structures and ship in ice. Ahmed.derradji-Aouat@nrc-cnrc.gc.ca